Harmonic assessment-based adjusted current total harmonic distortion

Shady H.E. Abdel Aleem[1], Ahmed M. Ibrahim[2], Ahmed F. Zobaa[3]

[1]*Mathematical, Physical & Life Sciences, 15th of May Higher Institute of Engineering, 15th of May City, Helwan, Cairo 11731, Egypt*
[2]*Electrical Power and Machines, Faculty of Engineering, Cairo University, Giza 12613, Egypt*
[3]*College of Engineering, Design and Physical Sciences, Brunel University London, Uxbridge, Middlesex UB8 3PH, UK*
E-mail: Shossam@theiet.org 20 1 2016

Published in *The Journal of Engineering*; Received on 7th January 2016; Revised on 20th January 2016; Accepted on 15th March 2016

Abstract: Power systems suffer from harmonic distortion and extra ohmic losses associated with them. Moreover, all harmonic frequencies are mostly assumed to have the same effect on the system losses. However, the frequency-dependency of the resistances should be taken into account, so that the apparent power and the power factor have to considerably reflect power losses under non-sinusoidal conditions. In this study, the difference between unweighted and weighted non-sinusoidal losses is addressed. A new harmonic-adjusted total harmonic distortion (THD) definition is proposed for both voltage and current. Besides, a new formula that relates the proposed harmonic-adjusted THD and a generalised harmonic derating factor definition of the frequency-dependent losses of the power transmission and distribution equipment is derived. An optimal ***C***-type passive filter design for harmonic mitigation and power factor correction based on the minimisation of the proposed harmonic-adjusted THD for a balanced non-sinusoidal system is introduced. A comparative study of the proposed filter design based on the new harmonic-adjusted definition, and a conventional filter design based on standard THD definition, is presented.

1 Introduction

The undesirable effects of non-sinusoidal conditions in a power system are usually related to the increase of the equipment losses. Nowadays, the structure of the power system networks continues its complication because of the growth of the distributed generation-based renewable energy technologies, and the advance in the use of non-linear loads. Thus, much attention should be paid to power system harmonic distortion to meet the present and future requirements of quality of electric power systems [1–5].

Most consumers think about mitigating the harmonic distortion only when they suffer from low-power factor and pay the price directly in cash or indirectly in technical problems caused by the ineffective use of their equipment because of the operation in a distorted non-sinusoidal environment. In this context, despite their different corresponding losses, an ampere drawn at any harmonic order is evaluated the same as the ampere drawn at the fundamental frequency. Furthermore, all harmonic frequencies are unreasonably assumed to have the same effect on the system losses [6]. The main possible reason is that most of the conventional methods of energy metering do not take into account harmonic distortion, and consequently harmonic distortion penalties and incentives may be underway in research, but are not applied yet in practice [7].

In the literature, the IEEE working groups on non-sinusoidal conditions have proposed a set of definitions for the electrical quantities applied in a distorted environment. For example, IEEE Standard 1459–2010 [8] decomposes apparent power (S) into two principal components: fundamental apparent power (S_1) and polluted or non-fundamental apparent power (S_N). S_N is an important quantity because it can be a reasonable indication of harmonic pollution; thus, it can be useful for introducing harmonic penalties or incentives if it is included in rate structures. This harmonic pollution assessment was intensely discussed in [8–10]. However, the frequency-dependent losses of the equipment were not explicitly addressed.

One of the milestone studies that addressed this problem, and introduced an evaluation of some rate structures from the standpoint of revenue and harmonics, was that presented in [11]. It proposed a generalised form of a harmonic-adjusted power factor (APF) besides the conventional displacement, distorted, and actual PF definitions. In general, APF depends on the weighting of the non-sinusoidal voltage and current vectors. In [11, 12], they had discussed the criteria of simplicity, ease of employment, compatibility, and encouraging mitigation of harmonic distortion based on using the harmonic-APF principal. Unfortunately, no agreement about the frequency-dependent weights of the non-sinusoidal voltage and current vectors has been reached. In this context, but for rotary machines and motor drives, authors between the 1970s and 1990s used certain loss factors that attempted to include the frequency dependence of losses such as [13] for microprocessor-based AC inverter drives and [14] for high-power industrial drives. Reference [14] was one of the milestone articles that suggest the use of total harmonic distortion (THD) at no load as a measure of performance of pulse-width modulation inverter fed drives, but not to measure the motor losses. However, these studies were mainly concerned with motor drives not the harmonic distortion mitigation in the grid.

Like so, Jeon [15] proposed a frequency domain-based power theory that has clarified a minimum loss condition of a power system having transmission lines with frequency-dependent resistances using effective voltage and current expressions, these definitions were depending on the effective resistance of voltage and current weights. According to [8, 15], an effective Thevenin resistance R_e can be calculated from the equality of losses of sinusoidal and non-sinusoidal power loss, which means it is considerably affected by current harmonic spectrum. Most of these studies, however, concluded that a corrected PF definition should be addressed, especially with the advance of non-linear loads and the existence of high-current transformer windings, induction motor rotors, and cables [16, 17].

Regarding the frequency-dependent weights, and based on the experience gained from these studies, three observations should be clear. First, harmonic voltages are extremely less than the fundamental voltage. Second, currents should be more sinusoidal than voltages because of the rough skin and proximity effects. Third, the weighting factor of the fundamental frequency should equal one for either voltage or current vectors. Accordingly, voltage weights may be set to any value within a range from 0 to 1 as introduced in [11]. Also, as a reasonable assumption, it may be possible to determine the current weighting, which is the central dilemma, and take its inverse as a voltage weighting as presented and discussed in [15]. Accordingly, in this paper, voltage and current weighted factors based on [15] are introduced. The difference between unweighted and weighted non-sinusoidal losses, is addressed, and modified formulas for the polluted apparent power and adjusted current and voltage THD expressions are derived.

In recent years, the use of C-type damped filter in industrial applications has been arisen mainly because of its capability to dampen resonance may occur [18]. Besides, it guarantees adequate high-pass filtering for high-order harmonics with reasonable attenuation of low-order harmonic frequencies [19–25] and it has low-power loss compared with the other typical passive filter configurations. Accordingly, in this paper, an optimal C-type passive filter design for a typical balanced industrial system that involves a group of linear and non-linear loads, cables, and a distribution transformer, working under non-sinusoidal conditions because of harmonic currents and background harmonic voltage distortion, is proposed.

The difference between minimising the standard total current harmonic distortion, and a proposed adjusted total current harmonic distortion that takes into account frequency-dependent line losses, is illustrated. Finally, a new relationship between the proposed adjusted total current harmonic distortion and a generalised harmonic derating factor (HDF) definition of the electric power system components in the system under study is derived.

Genetic optimisation system engineering tool (GOSET) is used as an optimisation technique for the filter constrained optimal design. It is a MATLAB-based code for solving optimisation problems using evolutionary algorithms, particularly those related to electric machinery, power electronics, power systems, and a variety of other engineering problems [26, 27].

2 Harmonic-adjusted THD definition

On the basis of [15], the effective voltage ($\boldsymbol{V}_{\rm e}$) and the effective current ($\boldsymbol{I}_{\rm e}$) weighted vectors are defined relative to the transmission losses that they are causing as follows

$$\boldsymbol{V}_{\rm e}=\left[\sqrt{\frac{r_{\rm reference}}{r_1}}V_1,\ \sqrt{\frac{r_{\rm reference}}{r_2}}V_2,\ \ldots,\ \sqrt{\frac{r_{\rm reference}}{r_h}}V_h\right] \tag{1}$$

$$\boldsymbol{I}_{\rm e}=\left[\sqrt{\frac{r_1}{r_{\rm reference}}}I_1,\ \sqrt{\frac{r_2}{r_{\rm reference}}}I_2,\ \ldots,\ \sqrt{\frac{r_h}{r_{\rm reference}}}I_h\right] \tag{2}$$

where h is the harmonic order presented and $r_{\rm reference}$ is a reference resistance that can be settled to any value. Hence, the apparent effective power ($S_{\rm e}$) can be defined as that clarified in [8, 15] for non-sinusoidal power systems, as follows

$$S_{\rm e}\equiv V_{\rm e}I_{\rm e} \tag{3}$$

Definitions of the apparent effective power, active power, and PF have the advantage of independence on the value of the reference resistance. However, to comply with other power theories of non-sinusoidal systems such as the classic single-phase theory and the Buchholz's theory [28, 29]; $r_{\rm reference}$ can be defined as the fundamental resistance of the Thevenin source, transmission line/cable, or any other series resistance can be found. Separating the fundamental values of the voltage and the current from the other harmonic components and choosing the reference resistance as the line fundamental resistance, will lead to the formulation of new definitions of harmonic-adjusted voltage THD ($\mathrm{THDV_{HA}}$), and harmonic-adjusted total current harmonic distortion ($\mathrm{THDI_{HA}}$) that was presented in the discussion of [12], as follows

$$V_{\rm e}^2=V_1^2+V_{\rm H}^2,\qquad V_{\rm H}=\sqrt{\sum_{h\succ 1}\left(\frac{r_1}{r_h}V_h^2\right)}=\sqrt{\sum_{h\succ 1}\left(k_h^vV_h^2\right)} \tag{4}$$

$$I_{\rm e}^2=I_1^2+I_{\rm H}^2,\qquad I_{\rm H}=\sqrt{\sum_{h\succ 1}\left(\frac{r_h}{r_1}I_h^2\right)}=\sqrt{\sum_{h\succ 1}\left(k_h^iI_h^2\right)} \tag{5}$$

so that

$$k_h^v=\frac{1}{k_h^i}=\frac{r_1}{r_h},\qquad r_1=r_{\rm reference} \tag{6}$$

Thus, one can define the harmonic-adjusted THD for both voltage and current as follows

$$\mathrm{THDV_{HA}}=\frac{V_{\rm H}}{V_1}=\frac{\sqrt{\sum_{h\succ 1}\left(k_h^vV_h^2\right)}}{V_1} \tag{7}$$

$$\mathrm{THDI_{HA}}=\frac{I_{\rm H}}{I_1}=\frac{\sqrt{\sum_{h\succ 1}\left(k_h^iI_h^2\right)}}{I_1} \tag{8}$$

Analysing the apparent effective power will lead to the materialisation of the harmonic-adjusted THD expressions as follows:

$$S_{\rm e}^2=V_1^2\left(1+\mathrm{THD}\,V_{\rm HA}^2\right)\times I_1^2\left(1+\mathrm{THDI_{HA}^2}\right),\qquad S_{\rm e}^2=S_1^2\left[1+\mathrm{THD}V_{\rm HA}^2+\mathrm{THDI_{HA}^2}+\left(\mathrm{THD}\,V_{\rm HA}^2\mathrm{THDI_{HA}^2}\right)\right] \tag{9}$$

Recalling the fact that current distortion is considerably higher than voltage distortion; (9) can be plainly written as follows

$$S_{\rm e}^2=S_1^2\left(1+\mathrm{THDI_{HA}^2}\right) \tag{10}$$

Another approximation for (9) concerning both $\mathrm{THD}V_{\rm HA}$ and $\mathrm{THDI_{HA}}$ can be found for weak grids in the case of the voltage distortion is comparable with the current distortion [16]. However, taking into consideration the decaying of the weights of the effective voltage vector given in (1) with the harmonics increase; (10) is used in this paper. Accordingly, a harmonic-APF expression can be given as

$$\mathrm{APF}=\frac{P_{\rm average}}{S_{\rm e}}=\frac{P_{\rm average}}{S_1\sqrt{1+\mathrm{THDI_{HA}^2}}} \tag{11}$$

Consequentially, one can reasonably assume that the average active power is equal to the fundamental one since contributions of harmonics above the fundamental to the average power are relatively small. This will lead to a direct relation between the APF and the displacement PF (DPF) expressions as follows

$$\mathrm{APF}=\frac{1}{\sqrt{1+\mathrm{THDI_{HA}^2}}}\left(\frac{P_1}{S_1}\right),\qquad \mathrm{APF}=\frac{1}{\sqrt{1+\mathrm{THDI_{HA}^2}}}\mathrm{DPF}=M_1\times\mathrm{DPF} \tag{12}$$

The latter equation is very close to the well-known equation defined in

[6, 16] that relates the actual PF to the displacement one, as given in (13)

$$\mathrm{PF} = \frac{1}{\sqrt{1+\mathrm{THDI}^2}}\mathrm{DPF} = M_2 \times \mathrm{DPF} \tag{13}$$

where THDI is the conventional current THD, M_1 and M_2 are multipliers that relate the different PF definitions. These multipliers can be used to calculate the other PF definitions from the measured DPF. Both multipliers will be equal only if the considered system is a sinusoidal system, i.e. $M_1 = M_2 = 1$. Furthermore, their values will considerably decrease with the increase of the percentage of the harmonic distortion. The following section will demonstrate a perspective use for the multiplier M_1.

In the literature, the harmonic-APF was first introduced in [30] because of the belief in finding a corrected expression for the PF that includes the effects of the non-sinusoidal losses and skin effects. In its general form, it is defined as follows

$$\mathrm{APF} = \frac{P_{\text{average}}}{\sqrt{\sum_{h=1}\left(\beta_h^v V_h^2\right)}\sqrt{\sum_{h=1}\left(\lambda_h^i I_h^2\right)}} \tag{14}$$

where β_h^v and λ_h^i are the hth weighting coefficients of the non-sinusoidal voltage and current, respectively. However, no agreement has been achieved regarding which of them is the most appropriate set of weights.

3 Harmonic derating factor-based adjusted current THD

Fig. 1 shows the Thevenin equivalent circuit of a power system at the non-linear load location. $\boldsymbol{V}_{\mathrm{S}}^h$ and $\boldsymbol{Z}_{\mathrm{S}}^h$ represent the background system voltage and Thevenin impedance, respectively. $\boldsymbol{Z}_{\mathrm{S}}^h$ can be measured by an impedance–frequency scan or calculated from short-circuiting test studies. $\boldsymbol{I}_{\mathrm{L}}^h$ and $\boldsymbol{Z}_{\mathrm{L}}^h$ represent the harmonic current source and linear load impedance, respectively. Furthermore, a power cable and a distribution transformer of the consumer have been connected in-between the point of common coupling (PCC_1), and the load bus, or PCC_2. They are represented by their hth harmonic impedances $\boldsymbol{Z}_{\mathrm{Cb}}^h$ and $\boldsymbol{Z}_{\mathrm{Tr}}^h$, respectively. It should be mentioned that a variable in bold means it is a complex one. One can define the effective impedance seen from the load bus by a series impedance $\boldsymbol{Z}_{\text{effective}}^h$; it can be given as shown in (15). Hence, one can define the reference resistance as the fundamental harmonic resistance and r_{h} as the hth resistance of the effective impedance $\boldsymbol{Z}_{\text{effective}}^h$ as given in (16)

$$\boldsymbol{Z}_{\text{effective}}^h = \boldsymbol{Z}_{\mathrm{S}}^h + \boldsymbol{Z}_{\mathrm{Cb}}^h + \boldsymbol{Z}_{\mathrm{Tr}}^h \tag{15}$$

$$r_{\text{reference}} = r_1 = \mathrm{Re}\left\{\boldsymbol{Z}_{\text{effective}}^{h=1}\right\},\ r_h = \mathrm{Re}\left\{\boldsymbol{Z}_{\text{effective}}^h\right\} \tag{16}$$

Under sinusoidal conditions, the total transmission and distribution power is given in (17), where I_{rated} is the rated root-mean-square (RMS) line current at the fundamental frequency. Conversely, one can define the rated current as the current carrying capability of the power cable or the transformer's rated current

$$P_{\text{loss}}^1 = I_{\text{rated}}^2 \times \mathrm{Re}\left\{\boldsymbol{Z}_{\mathrm{S}}^1 + \boldsymbol{Z}_{\mathrm{Cb}}^1 + \boldsymbol{Z}_{\mathrm{Tr}}^1\right\} = I_{\text{rated}}^2 \times r_1 \tag{17}$$

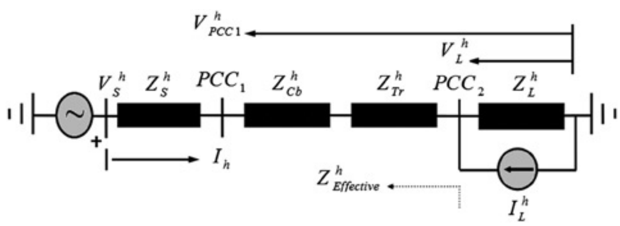

Fig. 1 *Thevenin equivalent circuit of a power system at the non-linear load location*

Under non-sinusoidal conditions, the total harmonic power loss is given in (18) where I_h represents the hth line current

$$P_{\text{loss}}^h = \sum_h I_h^2 \times \mathrm{Re}\left\{\boldsymbol{Z}_{\mathrm{S}}^h + \boldsymbol{Z}_{\mathrm{Cb}}^h + \boldsymbol{Z}_{\mathrm{Tr}}^h\right\} = \sum_h I_h^2 \times r_h \tag{18}$$

To get the value of a sinusoidal current that causes the same active power loss as the non-sinusoidal current, we can equate both losses as follows

$$I_{\text{rated}}^2 \times r_1 = \sum_{h=1}^{n} I_h^2 \times r_h \tag{19}$$

where n represents the maximum harmonic number presented. Dividing by r_1 and I_1^2, respectively

$$I_{\text{rated}}^2 = I_1^2 + I_2^2 \times \left[\frac{r_2}{r_1}\right] +,\ \ldots,\ I_n^2 \times \left[\frac{r_n}{r_1}\right] \tag{20}$$

$$\left(\frac{I_{\text{rated}}}{I_1}\right)^2 = 1 + \left(\frac{I_2}{I_1}\right)^2 \times \left[\frac{r_2}{r_1}\right] +,\ \ldots,\ \left(\frac{I_n}{I_1}\right)^2 \times \left[\frac{r_n}{r_1}\right] \tag{21}$$

Recalling [31], one can describe the harmonic content of the hth line current using the harmonic signature (HS) sequence as follows

$$\mathrm{HS} = \left(\alpha_1 = 1,\ \alpha_2 = \frac{I_2}{I_1},\ \ldots,\ \alpha_n = \frac{I_n}{I_1}\right) \tag{22}$$

where I_1 is the fundamental component of the current and $\alpha_1, \ldots, \alpha_n$ represent the nth per-unit HS of the current. Accordingly, substituting $\alpha_1, \ldots, \alpha_n$ in (21) we can find

$$\left(\frac{I_{\text{rated}}}{I_1}\right)^2 = 1 + \alpha_2^2 \times \left[\frac{r_2}{r_1}\right] + \cdots \alpha_n^2 \times \left[\frac{r_n}{r_1}\right] \tag{23}$$

The ratio I_1/I_{rated} represents a generalised HDF ($\mathrm{HDF_G}$) for the group composed of the electric power components under study. The $\mathrm{HDF_G}$ can indicate the effects of the non-sinusoidal losses. Hence, re-formulating (23), one can define the $\mathrm{HDF_G}$ as follows

$$\mathrm{HDF_G} = \frac{1}{\sqrt{1 + \sum_{h>1}^{n}\left(r_h/r_1\right)\alpha_h^2}} = \frac{1}{\sqrt{1 + \sum_{h>1}^{n} k_h^i \alpha_h^2}} \tag{24}$$

Therefore, based on the general HDF definition given in (24) and the harmonic-adjusted total harmonic current distortion given in (8), one can simply observe the following relation

$$\mathrm{HDF_G} = \frac{1}{\sqrt{1 + \mathrm{THDI}_{\mathrm{HA}}^2}} = M_1 \tag{25}$$

Consequentially, based on (25), one can deduce that both $\mathrm{THD_{HA}}$ is a mathematical expression that can be practiced as an indicator that can give a general view of the percentage of the harmonic derating may be required due to the non-sinusoidal currents and the total frequency-dependent losses in a distorted system.

4 *C*-type damped filters: theory and design

The *C*-type passive filters were first introduced in France–England high-voltage direct current project as a new filter for harmonic mitigation [21, 24]. However, only a few years ago, the *C*-filter begins to be a choice for the conventional single-tuned and high-pass filters for various industrial applications [18] because of its low-power loss, high capability of damping resonance, and reasonable attenuation of harmonics on a broad range of frequencies.

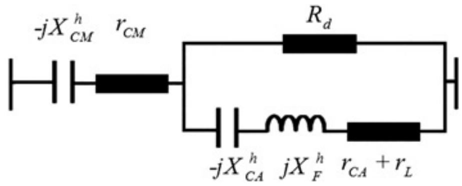

Fig. 2 *Schematic diagram of the C-type damped filter*

In general, the *C*-type filter is a high-pass filter plus an extra auxiliary capacitor, thus it has a similar frequency response to the high-pass filters. Fig. 2 shows a schematic diagram of the *C*-type filter. The auxiliary capacitive reactance (X_{CA}) is equal to the inductive reactance (X_F) at the fundamental frequency, thus short-circuiting the parallel resistor (R_d), reducing the fundamental power loss, and avoiding added voltage across the main capacitive reactance (X_{CM}). On the other side, the parallel resistor R_d will considerably reduce current amplifications and the increased harmonic distortion at resonance conditions. Consequentially, the high resonance damping capability of the *C*-type filters makes it applicable for situations when the harmonic pollution is not precisely known. For an accurate representation of the operating filter losses, equivalent series resistances for the capacitors (r_{CM}, r_{CA}) and an equivalent series resistance of the reactor (r_L), are shown in the schematic diagram. For a dielectric filled capacitor operating at 40°C, the loss is ~0.10 W/kvar. The power loss of the reactor can be represented by the X_F/r_L of the reactor, or the quality factor [19, 32].

On the basis of [21–24], sizing of the *C*-type filters' parameters can be introduced as given in (26)–(29), respectively, where *h* is the filter tuning number. Q_1 is the fundamental reactive power needed to improve the DPF to an acceptable value, f_1 is the fundamental frequency, and *m* is a damping factor varies between 1 and 20 [21, 22]. It should be noted that the capability of damping resonance increases as *m* decreases

$$C_M = \frac{Q_1}{2\pi f_1 V_1^2} \tag{26}$$

$$C_A = (h^2 - 1)C_M \tag{27}$$

$$L_F = \frac{V_1^2}{(h^2 - 1)2\pi f_1 Q_1} \tag{28}$$

$$R_d = m\frac{X_{CM}}{h} \tag{29}$$

5 System under study

5.1 Configuration and modelling of the system under study

Fig. 3 shows the equivalent circuit of the system under study. It consists of the following:

Utility-side: Represented by its Thevenin equivalent circuit where $\boldsymbol{V}_S^h$ is the *h*th harmonic background system voltage and $\boldsymbol{Z}_S^h$ is the *h*th harmonic short-circuit impedance that is given as

$$\boldsymbol{Z}_S^h = R_S^h + jX_S^h = [R_S^1 h^{0.5}] + j[X_S^1 h] \tag{30}$$

Consumer's cable: Represented by a series equivalent impedance $\boldsymbol{Z}_{Cb}$, where the cable capacitance is neglected because of its short length [17]. The *h*th cable impedance $\boldsymbol{Z}_{Cb}^h$ is given as shown in (31). Usually, the distribution lines and cables are represented by their exact equivalent π; however, an estimated correction factor for skin effect is applied by increasing the line resistance with frequency as suggested in [20, 33, 34]

$$\begin{aligned}\boldsymbol{Z}_{Cb}^h &= R_{Cb}^h + jX_{Cb}^h,\\ \boldsymbol{Z}_{Cb}^h &= [R_{Cb}^1(0.187 + 0.532h^{0.5})] + j[X_{Cb}^1 h], \quad h \ge 2.35\end{aligned} \tag{31}$$

Distribution transformer: Represented by a series equivalent impedance $\boldsymbol{Z}_{Tr}^h$ referred to its primary side so that the *h*th AC transformer resistance is divided into two resistances: a winding DC resistance $R_{Tr,dc}$ and the resistance $R_{Tr,ec}^h$ that correspond to the eddy-current losses [23], so that

$$\begin{aligned}\boldsymbol{Z}_{Tr}^h &= R_{Tr}^h + jX_{Tr}^h,\\ \boldsymbol{Z}_{Tr}^h &= [R_{Tr,dc} + h^2 R_{Tr,ec}] + j[X_{Tr}^1 h]\end{aligned} \tag{32}$$

Linear loads: Consist of a group of induction motors and other loads, they are represented by the *h*th impedance $\boldsymbol{Z}_L^h$ so that

$$\boldsymbol{Z}_L^h = R_L^1 + jX_L^h \tag{33}$$

Parts of these loads are individually compensated by a shunt capacitor represented by the *h*th capacitive reactance $-jX_C^h$.

Non-linear loads: Consist of a group of thyristor-DC drives, they are modelled as current sources $\boldsymbol{I}_L^h$ at the *h*th harmonic orders.

C-type damped filter: The proposed *C*-type filter represented by its simplified equivalent circuit at the non-linear loads' location.

$\boldsymbol{I}_h$ and $\boldsymbol{V}_h$ represent the *h*th harmonic current and voltage at the PCC, while $\boldsymbol{V}_L^h$ representing the *h*th harmonic voltage of the load bus. All are given by their RMS values as shown in (34)–(36), respectively, where $\boldsymbol{Z}_{LB}^h$ represents the parallel equivalent impedance of the load bus referred to the primary side of the transformer

$$\begin{aligned}\boldsymbol{I}_h &= \frac{\boldsymbol{V}_S^h + \boldsymbol{I}_L^h \boldsymbol{Z}_{LB}^h}{\boldsymbol{Z}_S^h + \boldsymbol{Z}_{Cb}^h + \boldsymbol{Z}_{Tr}^h + \boldsymbol{Z}_{LB}^h},\\ I &= \sqrt{\sum_h |I_h|^2}\end{aligned} \tag{34}$$

$$\begin{aligned}\boldsymbol{V}_h &= \boldsymbol{V}_S^h - \boldsymbol{I}_h \boldsymbol{Z}_S^h,\\ V &= \sqrt{\sum_h |V_h|^2}\end{aligned} \tag{35}$$

$$\begin{aligned}\boldsymbol{V}_L^h &= \boldsymbol{V}_h - \boldsymbol{I}_h(\boldsymbol{Z}_{Cb}^h + \boldsymbol{Z}_{Tr}^h),\\ V_L &= \sqrt{\sum_h |V_L^h|^2}\end{aligned} \tag{36}$$

5.2 Compensated system analysis

The different load PF expressions given in (37)–(39), respectively, will be used in analysing the system under study before and after compensation. A dot in bold indicates a scalar product. Consequentially, the standard THD THDV and THDI expressions, and the proposed adjusted THD $THDV_{HA}$ and $THDI_{HA}$ expressions, for both voltage and currents at the PCC, will be used for

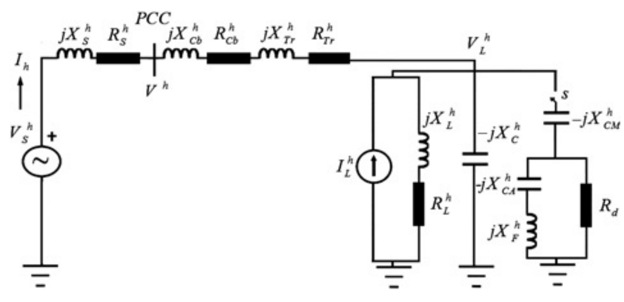

Fig. 3 *Configuration of the system under study*

doi: 10.1049/joe.2016.0002

assessing the harmonic distortion after reactive power compensation. Besides, the total three-phase transmission and distribution power losses P_{loss} is given in (40), the HDF of cables presented in [31] is expressed in (41) where I_{base} is the design RMS current of the cable

$$\mathrm{DPF} = \frac{\boldsymbol{V}_{\mathrm{L}}^{1} \cdot \boldsymbol{I}_{1}}{\boldsymbol{V}_{\mathrm{L}} \boldsymbol{I}} \tag{37}$$

$$\mathrm{PF} = \frac{\sum_{h} \left(\boldsymbol{V}_{\mathrm{L}}^{h} \cdot \boldsymbol{I}_{h} \right)}{V_{\mathrm{L}} I} \tag{38}$$

$$\mathrm{APF} = \frac{\sum_{h} \left(\boldsymbol{V}_{\mathrm{L}}^{\mathrm{h}} \cdot \boldsymbol{I}_{h} \right)}{\sqrt{\sum_{h=1} \left(k_{h}^{v} \left(V_{\mathrm{L}}^{h} \right)^{2} \right)} \sqrt{\sum_{h=1} \left(k_{h}^{i} I_{h}^{2} \right)}} \tag{39}$$

$$P_{\mathrm{loss}} = 3 \times \sum_{h} I_{h}^{2} \left(R_{\mathrm{S}}^{h} + R_{\mathrm{Cb}}^{h} + R_{\mathrm{Tr}}^{h} \right) \tag{40}$$

$$\mathrm{DF}_{\mathrm{Cb}} = \left(1 + \sum_{h>1} \left(\frac{R_{\mathrm{Cb}}^{h}}{R_{\mathrm{Cb}}^{1}} \right) \left(\frac{I_{h}}{I_{\mathrm{base}}} \right) \right)^{-0.5} \tag{41}$$

On the basis of IEEE Standard C57.110–2008 [35], a transformer's HDF $\mathrm{DF}_{\mathrm{Tr}}$ can be defined as [36]

$$\mathrm{DF}_{\mathrm{Tr}} = I_{\max}^{\mathrm{pu}} = \sqrt{\frac{1 + P_{\mathrm{EC-R}}^{\mathrm{pu}}}{1 + \left(F_{\mathrm{HL}} \times P_{\mathrm{EC-R}}^{\mathrm{pu}} \right)}} \tag{42}$$

where $\mathrm{P}_{\mathrm{EC-R}}^{\mathrm{pu}}$ is the per-unit winding eddy-current loss under rated conditions. F_{HL} is the per-unit harmonic loss factor for the winding eddy-currents, and it is defined as

$$F_{\mathrm{HL}} = \frac{\sum_{h} h^{2} \alpha_{h}^{2}}{\sum_{h} \alpha_{h}^{2}} \tag{43}$$

6 Optimisation problems under study

6.1 *Objective functions*

The two non-linear problem formulations that represent the proposed and the conventional optimal filter design approaches are expressed as shown below. Each objective function is formulated as a function of the variables X_{CM}, h, and m.

6.1.1 Proposed approach: Minimisation of the proposed adjusted total current harmonic distortion, or Min $\mathrm{THDI}_{\mathrm{HA}} = f_1 (X_{\mathrm{CM}}, h, m)$.

6.1.2 Conventional approach: Minimisation of the standard total current harmonic distortion, or Min $\mathrm{THDI} = f_2 (X_{\mathrm{CM}}, h, m)$.

6.2 *Constraints*

The previous objective functions are subject to the following non-linear constraints:

$0.9 \leq \mathrm{PF}\ (X_{\mathrm{CM}}, h, m) \leq 1$.
$0.95 \leq \mathrm{DPF}\ (X_{\mathrm{CM}}, h, m) \leq 1$.
$\mathrm{THDV}\ (X_{\mathrm{CM}}, h, m) \leq 5.00$.
$\mathrm{IHDV}\ (X_{\mathrm{CM}}, h, m) \leq 3.00$.
$\mathrm{THDI}\ (X_{\mathrm{CM}}, h, m) \leq 12.00$.
$\mathrm{IHDI}\ (X_{\mathrm{CM}}, h, m) \leq$ maximum IHDI.

where IHDV and IHDI are the individual harmonic voltage and current distortion in percentage, respectively. Both total and individual harmonic voltage distortion limits are specified for a voltage level <69 kV. Also, THDI and maximum IHDI limits are determined as defined in IEEE 519 tables for a short-circuit ratio <100 [37]. Besides, compliance of the capacitors with the shunt capacitor duties stated in IEEE Standard 18–2012 is taken into account [38] so that:

The RMS current of the capacitor $(X_{\mathrm{CM}}, h, m) \leq 1.35$ its rated value.
The RMS voltage of the capacitor $(X_{\mathrm{CM}}, h, m) \leq 1.1$ its rated value.
The peak voltage of the capacitor $(X_{\mathrm{CM}}, h, m) \leq 1.12$ its rated value.
The apparent power of the capacitor or its voltage–ampere $(X_{\mathrm{CM}}, h, m) \leq 1.35$ nameplate value.

6.3 *Search space*

The optimal size of parameters of the *C*-type filter corresponds to finding the global values of the three variables (X_{CM}, h, m). Accordingly, the search region is defined according to the boundaries defined for these variables. Regarding the main capacitive reactance X_{CM}, its lower and upper bounds are calculated knowing the set values of reactive power Q_1 needed to improve the DPF to its specified range and the fundamental phase-voltage, so that $X_{\mathrm{CM}} = V^2/Q_1$. The lower and upper boundaries of the tuning harmonic number h are considered to be 2 and 7. Besides, the lower and upper boundaries of the damping coefficient m are deemed to be 1–20.

The fitness value is an indication of merit for an individual. The higher (more positive) the fitness, the more optimal is an individual. Since the two problems are minimisation problems, hence, each fitness is taken as the inverse of the objective function plus a small positive number. Infeasible solutions (solutions that violate the constraints) are assigned with the value '−10' to reduce the chance of surviving in the population [26].

6.4 *Genetic optimisation system engineering tool*

Sudhoff presented a general purpose genetic algorithm package, a MATLAB-based code, which is called GOSET for solving single objective and multi-objective optimisation problems, particularly in power engineering applications. GOSET solves these problems using evolutionary algorithms; thus, it is very robust in its ability to seek global optimum rather than local optima. GOSET is a genetic algorithm package; thus, there is no considerable advantage

Table 1 Data of the system under study

Resistance	Value, Ω	Reactance	Value, Ω
R_{S}^{1}	0.0269	X_{S}^{1}	0.2688
R_{Cb}^{1}	0.5240	X_{Cb}^{1}	0.1659
$R_{Tr\_,\ dc}$	0.104	X_{Tr}^{1}	0.882
$R_{Tr,ec}^{1}$	0.024	X_{C}^{1}	132.30
R_{L}^{1}	14.9121	X_{L}^{1}	13.1226

Table 2 Harmonic contents of the supply voltage and the load current

h	V_{S}^{h}, *V*	I_{L}^{h}, *A*
5	55.00∠0°	21.6797∠−5 × 45°
7	40.00∠0°	18.7891∠−7 × 45°
11	35.00∠0°	15.8984∠−11 × 45°
13	30.00∠0°	11.5625∠−13 × 45°
17, 19, 23, 25	25.00∠0°	4.3359∠−*h* × 45°
29, 31, 35, 37	12.50∠0°	2.8906∠−*h* × 45°
41, 43, 47, 49	7.50∠0°	2.1680∠−*h* × 45°

Table 3 Uncompensated system results

Parameters	Original system
PF, %	73.03
DPF, %	82.69
APF, %	58.03
THDV, %	5.93
THDI, %	38.67
$THDI_{HA}$, %	95.27
F_{HL}, pu	12.36
DF_{Tr}, %	56.51
DF_{Cb}, %	85.55
HDF_G, %	72.40
P_{loss}, kW	76.81
Fixed capacitor duties with respect to the nominal values	
RMS voltage (%)	98.27
peak voltage (%)	143.12
RMS current (%)	260.62
volt–ampere (%)	255.98

in computation speed or accuracy compared with other genetic algorithm packages; however, GOSET is simpler. Readers may see [26] for more details on the GOSET package. It should be mentioned that typical values of the parameters of the GOSET algorithm are used in the search space.

7 Results and discussion

The test system, as shown in Fig. 3, was simulated using the GOSET optimisation package. The numerical data were taken from an example in [23], where the inductive three-phase loads are 1500 kW and 1320 kvar. The utility is represented by a 150 MVA short-circuit power, 60 Hz supply bus voltage of 6.35 kV (line-to-line), and $X_S/R_S = 10$.

The power cable used is trefoil formed, PVC insulated, unarmoured, single core copper wire, 35 mm^2 cross-sectional area, with a length of 1 km, and a fundamental design current of 185 A. The distribution transformer is a dry-type, star–star connected transformer with the nameplate ratings of 2 MVA and 6300 V/400 V, where its per-unit winding eddy-current loss under rated conditions is measured as 0.231 [23]. The reactive power supplied by the fixed capacitor bank is given as 100 kvar (per-phase).

Table 4 Simulation results of the compensated system

Parameters	Proposed approach	Conventional approach
X_{CM}, Ω	26.2322	26.2352
X_{CA}, Ω	1.0384	1.0948
X_F, Ω	1.0384	1.0948
R_d, Ω	10.2295	12.6751
PF, %	94.43	94.43
DPF, %	95.00	95.00
APF, %	92.58	92.45
THDV, %	2.64	2.70
THDI, %	10.43	9.85
$THDI_{HA}$, %	23.10	23.60
F_{HL}, pu	1.71	1.79
DF_{Tr}, %	93.97	93.33
DF_{Cb}, %	98.82	98.89
HDF_G, %	97.43	97.33
P_{loss}, kW	35.36	35.44
Fixed capacitor duties with respect to its nominal values		
RMS voltage, %	100.36	100.39
peak voltage, %	113.70	114.75
RMS current, %	116.88	120.81
volt–ampere, %	117.24	121.21
Main capacitor duties with respect to its nominal values		
RMS voltage, %	100.38	100.38
peak voltage, %	108.65	108.40
RMS current, %	104.40	104.17
volt–ampere, %	104.79	104.55

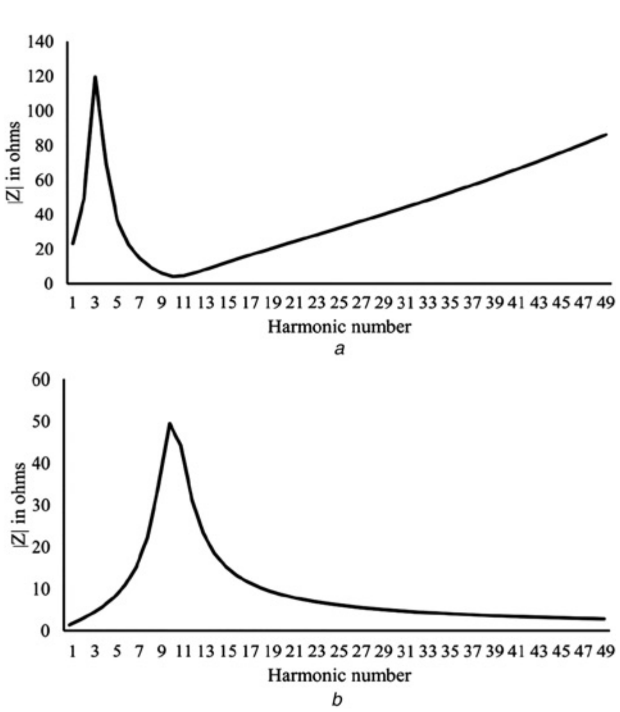

Fig. 4 *Equivalent impedance seen from the source and load sides, respectively*
a Equivalent impedance seen from the source side
b Equivalent impedance seen from the load side

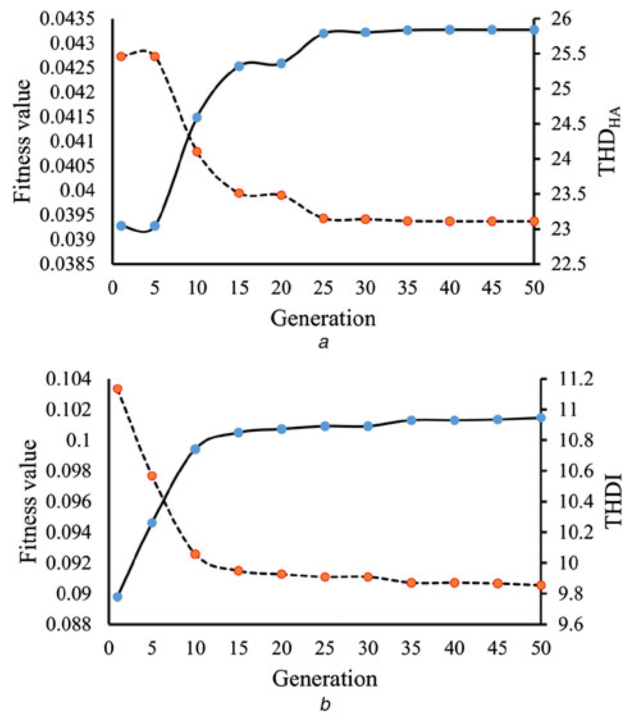

Fig. 5 *Improvement of the solutions (fitness and objective values) during the search algorithm*
a Proposed approach: minimisation of THD_{HA}
b Conventional approach: minimisation of THDI

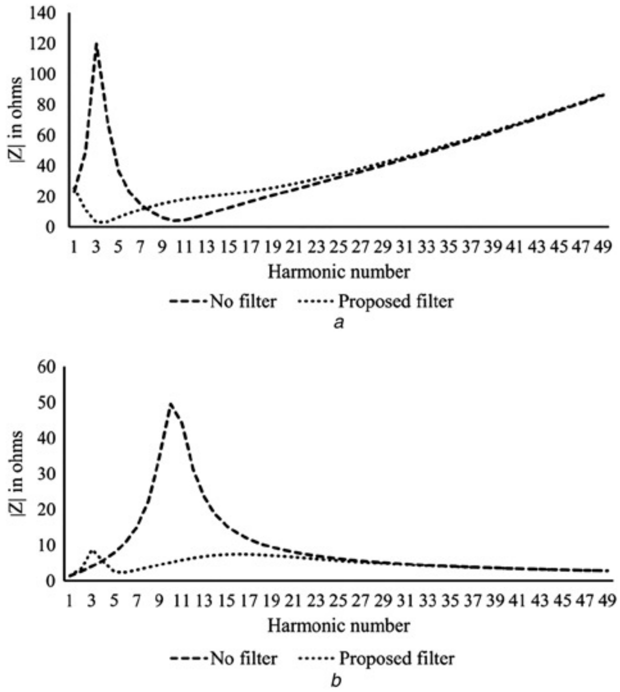

Fig. 6 *Equivalent impedance seen from the source and load sides before and after compensation, respectively*
a Equivalent impedance seen from the source side
b Equivalent impedance seen from the load side

Consequentially, the calculated system data for the equivalent single-phase mode is provided in Table 1. Harmonic components of single-phase background voltage and non-linear load current (referred to the primary side of the transformer) are given in Table 2. Also, the simulation results of the uncompensated system are shown in Table 3.

The simulation results for the uncompensated system indicate poor power quality indices. Both the transformer and the cable have low-current carrying capabilities, especially the transformer capability that is shown as 56.51%. Also, according to IEEE Standard 18–2012, the fixed capacitor duties indicate it is prone to a permanent failure. Besides, this severe violation in the percentages denotes a resonance occurrence as clarified in Fig. 4 for the equivalent impedance seen from the source and the load sides, respectively.

As verified in Fig. 4, resonance at the 11th harmonic number has occurred due to the inconsistent fixed capacitor bank. Accordingly, it was ascertained in this particular case that using a *C*-type damped filter is the viable solution.

The simulation results of the compensated system, with the optimal sizing of the proposed filters' parameters, are given in Table 4. Moreover, Fig. 5 shows the improvement of the objective functions and the fitness values versus the number of generations during the search algorithm for both proposed and conventional approaches, respectively.

The simulation results of the system with the proposed filters show a distinct improvement in the system performance compared with the outcome of the uncompensated system. Both approaches lead to significant reductions in the values of the THDV, THDI,

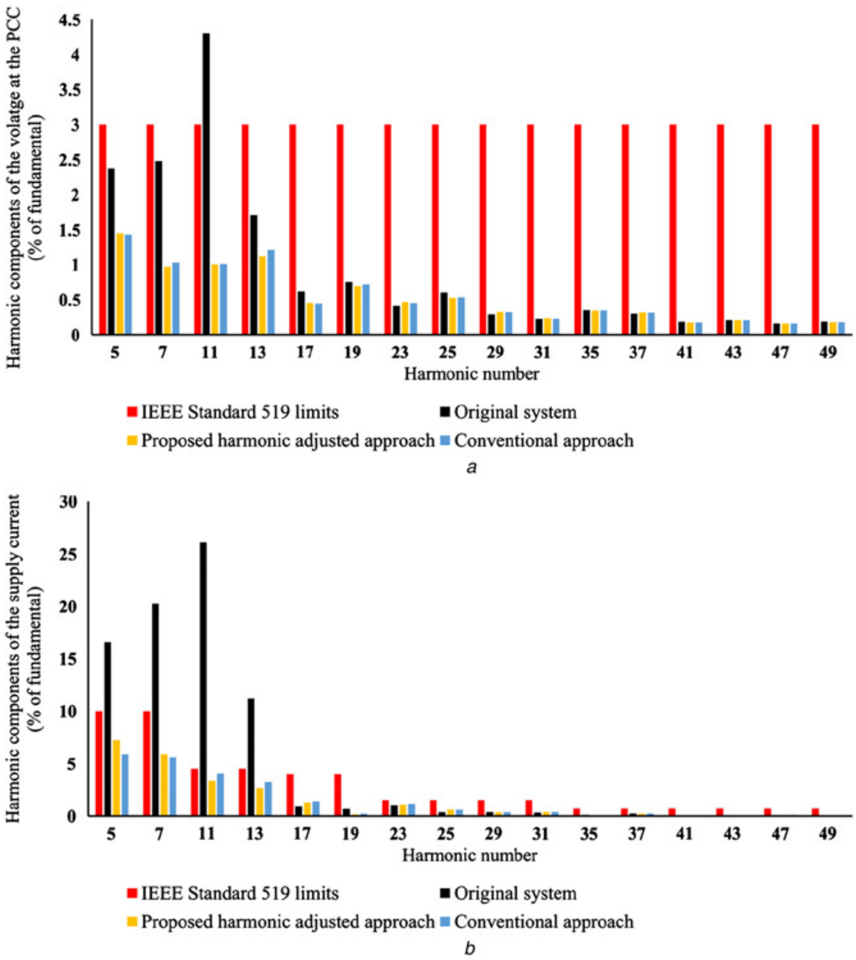

Fig. 7 *Harmonic contents of the voltage and the current measured at the PCC, before and after compensation, respectively*
a Harmonic content of the voltage at the PCC as a percentage of the fundamental component
b Harmonic content of the supply current as a percentage of the fundamental component

$THDI_{HA}$, F_{HL}, and P_{loss}, and an increase in the value of the APF while achieving the desired ranges of both the PF and the DPF. Additionally, high-current carrying capabilities of the transformer and the cable are obtained, indicating no need for derating them with the filter installed on the load side as validated by the values of the generalised HDF HDF_G. However, the power quality indices observed for the proposed approach are better than corresponding values observed for the conventional one, as shown in Table 4. The proposed method attains higher-current carrying capability and lower harmonic loss factor values for the transformer, higher HDF_G and APF, lower THDV, and lower transmission and distribution losses compared with the simulation results obtained with the conventional approach. On the other side, the value of the HDF of the cable observed for the conventional approach is marginally higher than the corresponding value observed for the proposed one [39].

Regarding the loading duties of the fixed and the main capacitors, Table 4 shows that all their values are well below the standard limits, for both approaches. This is validated as shown in Fig. 6 for the equivalent impedance seen from the source and the load sides after compensation. The uncompensated equivalent impedance values have been held in Fig. 6 for comparison purposes. Also, the impedance–frequency scan for both approaches is very similar; thus, only the impedance–frequency scan of the proposed approach is shown. The proposed *C*-type damped filter dampens the resonance as clarified in Fig. 6. Furthermore, Fig. 7 demonstrates that the harmonic contents of the voltage and current measured at the PCC for both approaches are complying with the limits of the IEEE 519. The main reason for the similar results between the two approaches because both methods minimise the current THD; however, the proposed use of the THD_{HA} has the advantage of indicating the non-sinusoidal losses in the system compared with the conventional THD definition, since it predicts the distortion in the current and subsequent additional losses which are typically the major issues in industrial applications.

As presented in this paper, the HDF_G can be practiced as an indicator that can give a general view of the percentage of the harmonic derating may be required due to the non-sinusoidal currents regarding the total frequency-dependent losses in a system. Remarkably, it can be used for harmonic pricing by re-adjusting a consumer's monthly bill, or introducing a harmonic distortion penalty. In simple words, assume the total monthly bill for an industrial firm is TB, which is calculated by a two-part tariff that is commonly used for industrial loads. It is based on measuring both the maximum demand (D_{max}) in kilowatts (kW) and the energy consumed in kWh. It is expressed as given in (44), where C_1 is the rate per kW of maximum demand and C_2 is the energy rate per kWh

$$\mathrm{TB} = \left(C_1 \times D_{\max}\right) + \left(C_2 \times E\right) \tag{44}$$

A harmonic-adjusted total monthly bill (TB_{HA}) can reasonably take the form suggested in (45), where (2-HDF_G) represents the harmonic pricing or the increase in the monthly bill (penalty) for the energy wasted due to the non-sinusoidal losses. The harmonic penalty should be applied if harmonic currents exceed the standard limits

$$\mathrm{TB}_{\mathrm{HA}} = \left[\left(C_1 \times D_{\max}\right) + \left(C_2 \times E\right)\right]\left(2 - \mathrm{HDF}_{\mathrm{G}}\right) \tag{45}$$

For example, the HDF_G of the uncompensated system was given as 72.40%. This means a 27.6% wasted capacity of the system, accordingly this consumer should be penalised by increasing its total monthly bill by the multiplier (2−0.724) or 1.276. It should be mentioned that a suggested multiplier was 1.33 in [12]. On the other hand, the HDF_G of the compensated system was given as 97.43%, for the proposed approach. This means a dramatic reduction in the wasted capacity of the system (2.57%). Thus, the HDF_G can be used as a harmonic rebate for large consumers following the standard limits. However, finding such a harmonic rate structure is an elaborate exercise that needs comprehensive techno-economic studies with updated energy policies. This point will be considered in future works.

8 Conclusion

In this paper, a new adjusted THD definition is proposed for both voltage and current. Besides, a new formula that relates the proposed adjusted current THD, and a generalised HDF that describes the frequency-dependent losses of the power transmission and distribution equipment, is derived. An optimal *C*-type damped passive filter design for harmonic mitigation and PF correction based on the minimisation of the proposed adjusted current THD for a balanced non-sinusoidal system is introduced. A comparative study of the proposed filter design based on the new harmonic-adjusted definition, and a conventional filter design based on standard THD definition, is presented. The simulation results demonstrate the viability of the proposed approach. The proposed set of currents' weighting coefficients reasonably increase the harmonics above the fundamental. Besides, the results indicate that the harmonic-adjusted-based derating factor guarantees lower harmonic loss factor values for the transformer, higher APF, and lower transmission and distribution losses compared with the simulation results based on conventional approaches. Furthermore, the perception of the generalised HDF can be applied in the case of unequal transmission line resistance in the three-phase mode. Finally, the performance and effectiveness of the proposed approach were verified by the various simulation results presented.

9 References

[1] Singh G.K.: 'Power system harmonics research: a survey', *Eur. Trans. Electr. Power*, 2009, **19**, (2), pp. 151–172, doi: 10.1002/etep.201

[2] Zobaa A.F., Aleem S.H.E.A.: 'A new approach for harmonic distortion minimization in power systems supplying nonlinear loads', *IEEE Trans. Ind. Inf.*, 2014, **10**, (2), pp. 1401–1412, doi: 10.1109/TII.2014.2307196

[3] Pena-Alzola R., Liserre M., Blaabjerg F., Ordonez M., Yang Y.: 'LCL-filter design for robust active damping in grid-connected converters', *IEEE Trans. Ind. Inf.*, 2014, **10**, (4), pp. 2192–2203, doi: 10.1109/TII.2014.2361604

[4] Wu J.-C., Jou H.-L., Hsaio H.-H., Xiao S.-T.: 'A new hybrid power conditioner for suppressing harmonics and neutral-line current in three-phase four-wire distribution power systems', *IEEE Trans. Power Deliv.*, 2014, **29**, (4), pp. 1525–1532, doi: 10.1109/TPWRD.2014.2322615

[5] Abdel Aleem S.H.E., Elmathana M.T., Zobaa A.F.: 'Different design approaches of shunt passive harmonic filters based on IEEE Standard 519–1992 and IEEE Standard 18–2002', *Recent Pat. Electr. Eng.*, 2013, **6**, (1), pp. 68–75, doi: 10.2174/2213111611306010009

[6] Grady W.M., Gilleskie R.J.: 'Harmonics how they relate to power factor'. EPRI Proc. of the Power Quality Issues & Opportunities Conf., San Diego, CA, November 1993, pp. 1–8

[7] Peng Y., Tao S., Xu Q., Xiao X.: 'Harmonic pricing model based on harmonic costs and harmonic current excessive penalty'. Second Int. Conf. on Artificial Intelligence, Management Science and Electronic Commerce (AIMSEC), Deng Leng, China, August 2011, pp. 4011–4014. doi: 10.1109/AIMSEC.2011.6009892

[8] IEEE standard definitions for the measurement of electric power quantities under sinusoidal, nonsinusoidal, balanced, or unbalanced conditions, in IEEE Standard 1459–2010 (Revision of IEEE Standard 1459–2000), March 19 2010, pp. 1–50, doi: 10.1109/IEEESTD.2010.5439063

[9] IEEE Working Group on Non-Sinusoidal Situations: 'Practical definitions for powers in systems with nonsinusoidal waveforms and unbalanced loads: a discussion', *IEEE Trans. Power Deliv.*, 1996, **11**, (1), pp. 79–101, doi: 10.1109/61.484004

[10] Emanuel A.E.: 'On the assessment of harmonic pollution', *IEEE Trans. Power Deliv.*, 1995, **10**, (3), pp. 1693–1698, doi: 10.1109/61.400958

[11] McEachern A., Grady W.M., Moncrief W.A., Heydt G.T., McGranaghan M.: 'Revenue and harmonics: an evaluation of some proposed rate structures', *IEEE Trans. Power Deliv.*, 1995, **10**, (1), pp. 474–482, doi: 10.1109/61.368364
[12] Arseneau R., Heydt G.T.: 'Application of IEEE standard 519–1992 harmonic limits for revenue billing meters', *IEEE Power Eng. Rev.*, 1997, **17**, (1), p. 57, doi: 10.1109/MPER.1997.560700
[13] Handley P.G., Boys J.T.: 'Practical real-time PWM modulators: an assessment', *IEE Proc. B, Electr. Power Appl.*, 1992, **139**, (2), pp. 96–102, doi: 10.1049/ip-b.1992.0013
[14] Stemmler H.: 'High-power industrial drives', *Proc. IEEE*, 1994, **82**, (8), pp. 1266–1286, doi: 10.1109/5.301688
[15] Jeon S.-J.: 'Non-sinusoidal power theory in a power system having transmission lines with frequency-dependent resistances', *IET Gener. Trans. Distrib.*, 2007, **1**, (2), pp. 331–339, doi: 10.1049/iet-gtd:20050446
[16] Emanuel A.E.: 'Power definitions and the physical mechanism of power flow' (John Wiley, Hoboken, NJ, USA, 2010)
[17] Abdel Aleem S.H.E., Balci M.E., Zobaa A.F., Sakr S.: 'Optimal passive filter design for effective utilization of cables and transformers under non-sinusoidal conditions'. Proc. 16th Int. Conf. Harmonics and Quality of Power (ICHQP'14), Bucharest, Romania, May 2014, pp. 626–630, doi: 10.1109/ICHQP.2014.6842881
[18] Xu W., Ding T., Li X., Liang H.: 'Resonance-free shunt capacitors – configurations, design methods and comparative analysis', *IEEE Trans. Power Deliv.*, 2016, **PP**, (99), p. 1, doi: 10.1109/TPWRD.2015.2507440
[19] Das J.C.: 'Power system harmonics and passive filter design' (Wiley-IEEE Press, Hoboken, NJ, USA, 2015, 2nd edn.)
[20] Arrillaga J., Watson N.R.: 'Power system harmonics' (Wiley, Chichester, UK, 2013, 2nd edn.)
[21] Xiao Y., Zhao J., Mao S.: 'Theory for the design of C-type filter'. Proc. 11th Int. Conf. Harmonics and Quality of Power (ICHQP'04), Lake Placid, New York, September 2004, pp. 11–15. doi: 10.1109/ICHQP.2004.1409321
[22] Aravena P., Vallebuona G., Moran L., Dixon J., Godoy O.: 'Passive filters for high power cycloconverter grinding mill drives'. Industry Applications Society Annual Meeting (IAS'09), Houston, TX, October 2009, pp. 1–7. doi: 10.1109/IAS.2009.5324939
[23] Balci M.E.: 'Optimal C-type filter design to maximize transformer's loading capability under non-sinusoidal conditions', *Electric Power Components & Systems*, 2014, **42**, (14), pp. 1565–1575. doi: 10.1080/15325008.2014.943827
[24] Abdel Aleem S.H.E., Zobaa A.F., Abdel Aziz M.M.: 'Optimal C-type passive filter based on minimization of the voltage harmonic distortion for nonlinear loads', *IEEE Trans. Ind. Electron.*, 2012, **59**, (1), pp. 281–289. doi: 10.1109/TIE.2011.2141099
[25] Mohamed I.F., Abdel Aleem S.H.E., Ibrahim A.M., Zobaa A.F.: 'Optimal sizing of C-type passive filters under non-sinusoidal conditions', *Energy Technol. Policy*, 2014, **1**, (1), pp. 35–44, doi: 10.1080/23317000.2014.969453
[26] Sudhoff S.D.: 'Genetic optimization system engineering toolbox (GOSET: version 2.6)' (School of Electrical and Computer Engineering, Purdue University, 2014). Available at https://www.engineering.purdue.edu/ECE/Research/Areas/PEDS/go_system_engineering_toolbox
[27] Sudhoff S.D.: 'Power magnetic devices: a multi-objective design approach' (IEEE-Press/Wiley, Hoboken, NJ, USA, 2014)
[28] Akagi H., Watanbe E.H., Aredes M.: 'Instantaneous power theory and applications to power conditioning' (IEEE Press/Wiley-Interscience, Hoboken, NJ, USA, 2007)
[29] Buchholz F.: 'Apparent power in unbalanced three-phase systems', *Licht Kraft, Z. Elektr. Energ.-Nutzung*, 1922, **2**, pp. 9–11
[30] McEachern A., Grady W.M.: 'Harmonic adjusted power factor meter', U.S. Patent 5212441, May 1993
[31] Hiranandani A.: 'Calculation of cable ampacities including the effects of harmonics', *IEEE Trans. Ind. Appl. Mag.*, 1998, **4**, (2), pp. 42–51, doi: 10.1109/2943.655660
[32] Pinceti P., Prando D.: 'Sensitivity of parallel harmonic filters to parameters variations', *Electr. Power Energy Syst.*, 2015, **68**, pp. 26–32, doi: 10.1016/j.ijepes.2014.12.030
[33] Riberio P.F.: 'Tutorial on harmonics modeling and simulation'. Proc. IEEE Power Engineering Society Winter Meeting, Tampa, FL, US, February 1998
[34] Kocewiak L.H., Hjerrild J., Bak C.L.: 'Wind farm structures' impact on harmonic emission and grid interaction'. The European Wind Energy Conf. & Exhibition, EWEC 2010, Warszawa, Poland, April 2010
[35] IEEE Recommended Practice for Establishing Liquid-Filled and Dry-Type Power and Distribution Transformer Capability When Supplying Nonsinusoidal Load Currents - Redline, in IEEE Std C57.110–2008 (Revision of IEEE Std C57.110–1998) - Redline, Aug. 15 2008, pp.1–67
[36] Masoum M.A.S., Moses P.S., Masoum A.S.: 'Derating of asymmetric three-phase transformers serving unbalanced nonlinear loads', *IEEE Trans. Power Deliv.*, 2008, **23**, (4), pp. 2033–2041, doi: 10.1109/TPWRD.2008.923057
[37] IEEE recommended practice and requirements for harmonic control in electric power systems, in IEEE Standard 519–2014 (Revision of IEEE Standard 519–1992), June 11 2014, pp. 1–29, doi: 10.1109/IEEESTD.2014.6826459
[38] IEEE standard for shunt power capacitors, in IEEE Standard 18–2012 (Revision of IEEE Standard 18–2002), February 15 2013, pp. 1–39, doi: 10.1109/IEEESTD.2013.6466331
[39] Abdel Aleem S.H.E., Balci M.E., Sakr S.: 'Effective utilization of cables and transformers using passive filters for non-linear loads', *Int. J. Electr. Power Energy Syst.*, 2015, **71**, pp. 344–350, doi: 10.1016/j.ijepes.2015.02.036